Hydrogen Bonds

DOI: 10.1002/ange.201100469

A Biologically Relevant Co^{1+}···H Bond: Possible Implications in the Protein-Induced Redox Tuning of Co^{2+}/Co^{1+} Reduction**

*Manoj Kumar and Pawel M. Kozlowski**

Methyltransferases[1–3] (e.g., methionine synthase (MetH),[1] methanol-cobalamin methyltransferase (MtaBC),[2] or corrinoid/Fe-S protein (CFeSP)[3]) and ATP:cob(I)alamin adenosyltransferases (ACA)[4,5] differ vastly in their catalytic functioning, yet a common thread connects these two seemingly different classes of enzymes, namely, reduction of cob(II)alamin (Co^{2+}Cbx) to cob(I)alamin (Co^{1+}Cbx) serves as one of the key components of their catalytic cycles. The Co^{2+}/Co^{1+} reduction is a thermodynamically challenging reaction because the midpoint reduction potentials of the physiological reducing agents (−260 to −440 mV versus the standard hydrogen electrode (SHE)) are considerably more positive than that of the unbound Co^{2+}Cbx intermediate (−500 mV vs. SHE as measured in water solution).[6–8] But this reaction is indeed observed when the enzyme-bound Co^{2+}Cbx is considered, thus implying that the enzyme must be exercising subtle mechanistic control over the reduction process. In spite of being a ubiquitous chemical event, detailed mechanistic insight into how Co^{2+}/Co^{1+} reduction is accomplished inside the enzymes has yet to be fully revealed.

Based on spectroscopic[9–12] and X-ray structure studies,[5,13] the generation of tetracoordinated Co^{1+}Cbx has been invoked to be the key molecular determinant of the enzyme-mediated redox tuning of the Co^{2+}/Co^{1+} process. The reduction event in the case of human-type ACA is even postulated to be mediated by tetracoordinated Co^{2+}Cbx.[5,11,12] However, the possibility of pentacoordinated Co^{2+}Cbx displaying weak axial interactions has not been ruled out. In the case of MetH enzyme, the reduction process has been suggested to proceed via pentacoordinated Co^{2+}Cbx wherein the role of active-site interaction, especially that of the Y1139 residue, has been assessed of catalytic importance in weakening the interaction between the cofactor and β ("upper") axial ligand (H_2O), which in turn will promote the reduction process.[10,13]

However, an alternative catalytic strategy for driving Co^{2+}/Co^{1+} reduction can be envisioned if we take into account recent studies on Pt^{2+}···H bonds,[14,15] for which it has been shown that the filled d orbitals of square-planar d^8 metal ions can also serve as H-bond acceptors. A number of square-planar Pt^{2+} compounds exhibiting X−H···Pt^{2+} (X = N, C or O) weak interactions have been structurally identified.[16–18] The existence of a dispersion-driven O−H···Pt^{2+} interaction has been verified by using a low-temperature (20 K) neutron diffraction technique.[15]

Considering that the ground-state electronic structure of Co^{1+}Cbx also has a dominant component corresponding to a closed-shell d^8 configuration,[19,20] an interesting question arises of whether a Co^{1+} ion can also engage in metal-ion-based H-bond formation through its filled d orbitals. And if this is the case, what could be the implications of such associative interactions in relation to the Co^{2+}/Co^{1+} reduction process, a key catalytic conversion in a large variety of methyltransferases and adenosyltransferases?

Taking into account that Co^{1+}Cbx has only been spectroscopically characterized,[9] we turned our attention to computational modeling. To address whether Co^{1+}Cbx can form an H-bond with an axial ligand, simplified (Co^{1+}Cbl) as well as full structural (Co^{1+}Cbi) models of the Co^{1+}Cbx extracted from the high-resolution X-ray crystal structure of isolated Co^{2+}Cbx[21] were employed, wherein a H_2O molecule was placed on their β faces (Co^{1+}Cbl-OH_2; Co^{1+}Cbi-OH_2) to mimic the axial ligand (see Computational Details in the Supporting Information). To analyze whether the analogous Co^{2+}Cbx complexes would also form metal-ion-induced H-bonds, two different types of Co^{2+}Cbx complexes were considered: 1) pentacoordinated Co^{2+}Cbx wherein two commonly suggested conformations, namely (Co^{2+}Cbl···OH_2; Co^{2+}Cbi···OH_2) and (Co^{2+}Cbl···Im; Co^{2+}Cbi···Im),[22] were explored; and 2) hexacoordinated Co^{2+}Cbx (H_2O···Co^{2+}Cbl···Im;H_2O···Co^{2+}Cbi···Im) wherein H_2O and imidazole (Im) were modeled as β and α axial ligands, respectively. Since dispersion interactions cannot be correctly described using conventional DFT functionals, we also applied dispersion-corrected B97-D[23] and ωB97X-D[24] functionals in addition to BP86,[25,26] B97-1,[27,28] B98,[29] and ωB97X[30] functionals.

As is clear from Figures S1–S6 in the Supporting Information, the axial H_2O and Im ligands were O- and N-bound to the Co^{2+} ion in the optimized Co^{2+}Cbx complexes (Supporting Information, Tables S1–S6). Note here that the axial H_2O ligand in the H_2O···Co^{2+}Cbi···Im was significantly displaced (ca. 4.00–4.30 Å) away from the Co^{2+} ion, which indicates that the H_2O···Co^{2+}Cbi···Im complex is effectively a pentacoordinated complex. On the other hand, the H_2O ligand in the Co^{1+}Cbx complexes (Co^{1+}Cbl···**H**-O-H; Co^{1+}Cbi···**H**-O-H) was ligated to the Co^{1+} ion through its **H**-end (see Figure 1 and the Supporting Information, Tables S7 and S8), which implies that the tendency to form H-bonds is only mandated by d^8 metal ions. The Co^{1+}···**H**-O motif in the optimized Co^{1+}Cbl···**H**-O-H and Co^{1+}Cbi···**H**-O-H complexes was found

[*] M. Kumar, Prof. P. M. Kozlowski
Department of Chemistry, University of Louisville
2320 South Brook Street, Louisville, KY 40292 (USA)
E-mail: pawel@louisville.edu

[**] We acknowledge exceptional computational support provided by the Cardinal Research Cluster, University of Louisville.

Supporting information for this article is available on the WWW under http://dx.doi.org/10.1002/anie.201100469.

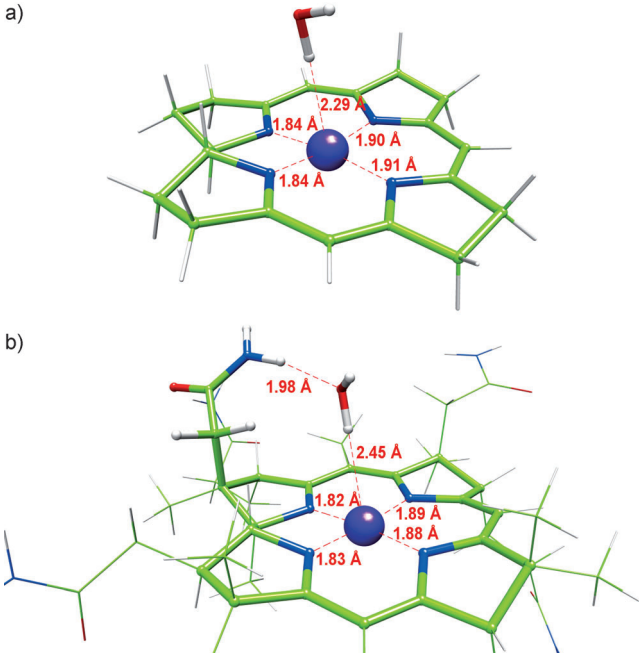

Figure 1. Close-ups of BP86-optimized H-bonded Co^{1+}Cbx complexes, wherein the regions of interest are highlighted using ball-and-stick representation. a) Co^{1+}Cbl···**H**-O-H (simplified); b) Co^{1+}Cbi···**H**-O-H (full).

to be almost linear, a structural feature ($\measuredangle M^{n+}$···**H**-X greater than 110°) that has usually been associated with **H**-bond-forming complexes.[31] Notably, the **H**–O bond of the H_2O axial ligand was found to be slightly lengthened relative to its H–O bond that supported the development of the Co^{1+}···**H** bond. The BP86-calculated harmonic vibrational frequencies further aided the elongation of the **H**–O bond, as the **H**–O stretching vibration (3328, 3352 cm^{-1}) was lower in energy than the H–O vibration (3747, 3670 cm^{-1}) in the **H**-bonded complexes. The Wiberg bond indices[32] that probe for covalent interactions afforded useful quantitative information to complement the Co^{1+}···**H** bond formation. The **H**–O bond had a lower bond index (0.711; 0.676) than the H–O bond (0.767; 0.761) whereas the Co^{1+}···**H** bond had a noticeable bond order of (0.040; 0.085), which signified the bonding interaction between the Co^{1+} ion and **H**–O motif of the H_2O axial ligand.

To validate the stability of the Co^{1+}···**H** bond, the static thermodynamic data for the complex formation (Co^{1+}Cbl···**H**-O-H; Co^{1+}Cbi···**H**-O-H) reaction was evaluated. Surprisingly, in the case of the Co^{1+}Cbl···**H**-O-H complex, the reaction was found to be nonspontaneous when studied using Hartree–Fock (HF) or conventional DFT functionals (BP86, B97-1, B98) with the exception of ωB97X (Figure 2 and Supporting Information, Table S9). This is in line with an earlier study,[9] which suggested that such complex formation (Co^{1+}Cbl···H_2O) is not possible from a thermodynamic point of view ($\Delta G = +1.96$ kcal mol^{-1}). However, when the thermodynamics of the complex was addressed using dispersion-corrected DFT, complex formation was found to be a spontaneous phenomenon with the B97-D functional, while the exothermic effect noticed with the ωB97X functional was

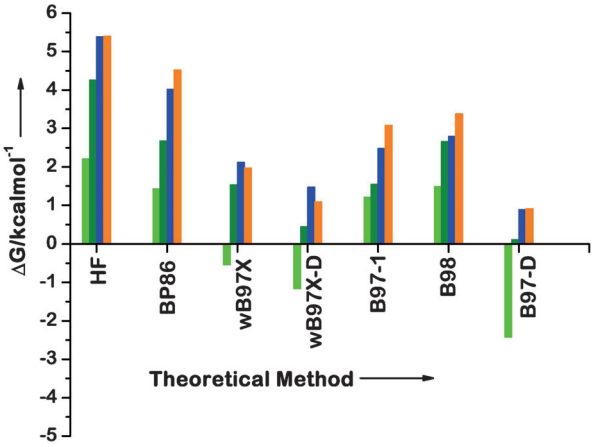

Figure 2. Computed Gibbs energy data for the Co^{1+}Cbl···**H**-O-H complex (green: gas phase, olive: chloroform, violet: acetonitrile, orange: water).

enhanced by about 1–2 kcal mol^{-1} upon inclusion of dispersion interactions with this functional. This result indicates that the dispersion component of the Co^{1+}···**H** linkage contributes noticeably towards the thermodynamic stability of the Co^{1+}Cbl···**H**-O-H complex. The importance of dispersion-corrected DFT has recently been illustrated in the case of transition-metal complexes[33] and carbene–carbene complex formation reactions.[34]

On the other hand, Co^{1+}···**H** bond formation in the case of the Co^{1+}Cbi···**H**-O-H complex was predicted to be an exothermic event at all levels of theory (Supporting Information, Figure S7 and Table S13). Note that although the Co^{1+}···H bond in the Co^{1+}Cbi···**H**-O-H complex was weaker than that in Co^{1+}Cbl···**H**-O-H (Figure 1), a relatively higher degree of exothermic effect was achieved in this case, which mainly resulted from the larger size of the cofactor (Co^{1+}Cbi) and an additional H-bond (-N–H···OH_2 = 1.98 Å) that the axial H_2O ligand forms with one of the amide side chains of the cofactor (Figure 1).

To assess the stability of the Co^{1+}···**H** linkage, the Co^{1+}Cbl···**H**-O-H and Co^{1+}Cbi···**H**-O-H complexes were solvated with chloroform ($\varepsilon = 4.7$), acetonitrile ($\varepsilon = 37$), and water ($\varepsilon = 78$) solvents (Figure 2 and Supporting Information, Figure S7, Tables S10–S12 and S14–S16). The solvated Co^{1+}···**H** bond was found to be appreciably destabilized with a lesser effect being noticed in the case of less polar solvent. The highly endothermic nature of the Co^{1+}···**H** bond in water also indicates why no such H-bond has been observed experimentally.[35] In spite of the weakening of the Co^{1+}···**H** linkage upon solvation, the Co^{1+}Cbl···**H**-O-H complex formation reaction, when studied using the B97-D and ωB97X-D functionals, was found to be essentially a thermoneutral event ($\Delta G = +0.18$–0.59 kcal mol^{-1}) in chloroform, an approximate solvent mimick of protein environment. On the other hand, the solvated Co^{1+}Cbi···**H**-O-H complex in chloroform solvent remained a thermodynamically stable entity at all DFT levels. The solvent-induced destabilization of the Co^{1+}···**H** linkage indicated that the Co^{1+}···**H** bond is a weaker interaction than the H_2O···H_2O H-bond.

The existence of the stable Co^{1+}···**H** bond was further supported by the minima observed on the interaction energy curves of the Co^{1+}Cbl···**H**-O-H and Co^{1+}Cbi···**H**-O-H complexes computed along the Co^{1+}–O coordinate (Supporting Information, Figure S8). The interaction energies of the **H**-bonded complexes were calculated as the difference between the total energies of the complexes (Co^{1+}Cbl···**H**-O-H; Co^{1+}Cbi···**H**-O-H) and the sum of the total energies of their separated monomers (Co^{1+}Cbl, H_2O; Co^{1+}Cbi, H_2O). The occurrence of the HF minima further pointed out the electrostatic nature of the Co^{1+}···**H** bond, while the deeper minima observed with DFT (BP86, B97-1, B98, B97-D, ωB97X, and ωB97X-D) functionals implied that the Co^{1+}···**H** bond also has dispersion and correlation contributions.

To further characterize the nature of the Co^{1+}···**H** interaction, atoms in molecules (AIM) analysis[36] was performed on the BP86-optimized geometries of the **H**-bonded complexes. In the AIM methodology, the topological properties of the electron density associated with the bond critical point (BCP) are analyzed to define the bond path that connects the interacting atoms. Within the formalism of AIM theory, the sign of total energy density ($H = G + V$) at a BCP is used as an instructive parameter to classify the bonding type, that is, whether the interaction is purely electrostatic ($H > 0$) or partially covalent ($H < 0$). For Co^{1+}···**H** interactions in the Co^{1+}Cbl···**H**-O-H and Co^{1+}Cbi···**H**-O-H complexes, the BCP could be located. Table S17 in the Supporting Information contains all the relevant BCP properties of Co^{1+}···**H** interactions. The Co^{1+}···**H** interaction in the Co^{1+}Cbl···**H**-O-H complex was found to be partially covalent in nature ($H = -0.00092$), whereas it was purely electrostatic ($H = +0.00094$) in the Co^{1+}Cbi···**H**-O-H complex thereby implying that the Co^{1+}···**H** interaction was stronger in the case of the Co^{1+}Cbl···**H**-O-H complex. This is also reflected in terms of the Co^{1+}···**H** bond distances depicted in Figure 1. This analysis further emphasized that the greater extent of exothermicity noticed in the case of the Co^{1+}Cbi···**H**-O-H complex was largely a result of its steric bulk and an additional binding interaction between the axial H_2O ligand and the amide side chain of the cofactor.

To gain insight into the electronic structure of the **H**-bonded complexes and to evaluate the role of orbital interaction between the Co^{1+} ion and H_2O ligand in stabilizing the Co^{1+}···**H** interaction, natural bond orbital (NBO) second-order perturbation analysis[37] was carried out on the BP86-optimized geometries of the Co^{1+}Cbl···**H**-O-H and Co^{1+}Cbi···**H**-O-H complexes. The calculated stabilization energy (5.62; 10.43 kcal mol^{-1}) due to the $n_{Co^{1+}}$ (filled d orbitals of Co^{1+} ion)→$\sigma^*_{\mathbf{H}-O}$ orbital interactions was significantly higher than that estimated for the $n_{Co^{1+}} \rightarrow \sigma^*_{H-O}$ interactions (0.82; 0.17 kcal mol^{-1}). This indicated a sizeable contribution of the metal-to-ligand charge-transfer component in the Co^{1+}···**H** linkage that was also reflected in the orbital occupancies of the $\sigma^*_{\mathbf{H}-O}$ (0.03; 0.06) and σ^*_{H-O} (0.00; 0.00) orbitals (Supporting Information, Table S18). Owing to the availability of metal antibonding orbitals ($n^*_{Co^{1+}}$) and an **H**–O bonding orbital ($\sigma_{\mathbf{H}-O}$) of appropriate symmetry and energy, the ligand-to-metal charge transfer also contributed towards the stabilization of the Co^{1+}···**H** bond, though its impact was relatively less. The role of such orbital interactions in stabilizing noncovalent Se···N,[38] Se···O,[39] and Se···F[40] linkages is well documented in the literature.

Considering that the present calculations predict a stable Co^{1+}···H bond that has charge-transfer, correlation, dispersion, and electrostatic contributions, an interesting question arises as to how it might impact the Co^{2+}/Co^{1+} reduction, a key step in many enzymatic reactions. Earlier studies[5,9–13] indicate that the generation of tetracoordinated Co^{1+}Cbx is required to facilitate thermodynamically challenging Co^{2+}/Co^{1+} reduction. But our computations suggest that Co^{1+}Cbx can indeed be pentacoordinated because of Co^{1+}···H bond formation. Thus, to quantify the possible catalytic effect of the Co^{1+}···**H** interaction, the reduction potentials for (Co^{2+}Cbl···OH_2/Co^{1+}Cbl; Co^{2+}Cbi···OH_2/Co^{1+}Cbi) and (Co^{2+}Cbl···OH_2/Co^{1+}Cbl···H_2O; Co^{2+}Cbi···OH_2/Co^{1+}Cbi···H_2O) couples were computed using our recently calibrated computational protocol (BP86/6-31 + G*) that predicts the reduction potentials of B_{12} cofactors with a reliable degree of accuracy (Figure 3).[41] A significant amount of redox tuning (ca. 100–225 mV vs. SHE) was

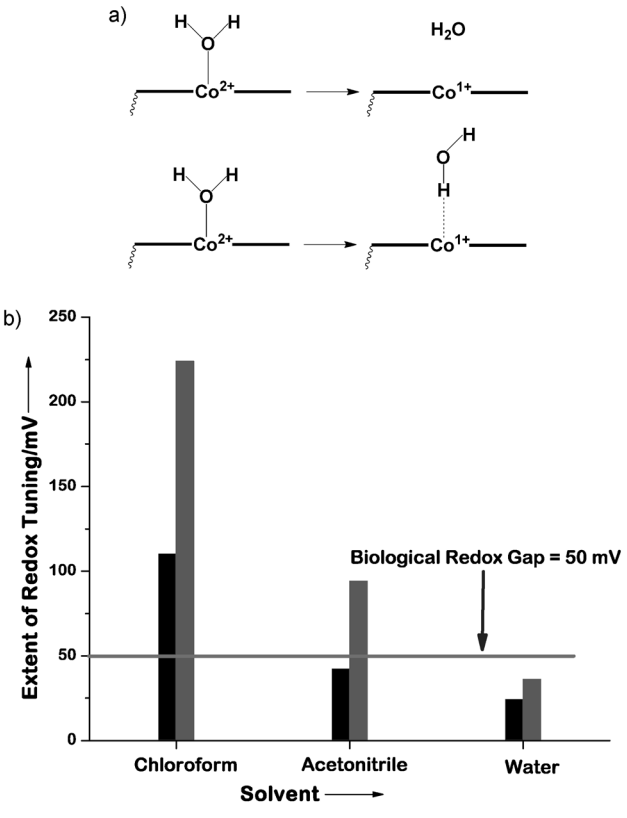

Figure 3. Co^{1+}···**H** interaction-induced redox tuning (versus SHE) of the Co^{2+}/Co^{1+} process. a) The studied reduction processes. b) Redox tuning computed as the difference between the reduction potentials of (Co^{2+}Cbl···OH_2/Co^{1+}Cbl; Co^{2+}Cbi···OH_2/Co^{1+}Cbi) and (Co^{2+}Cbl···OH_2/Co^{1+}Cbl···H_2O; Co^{2+}Cbi···OH_2/Co^{1+}Cbi···H_2O) couples (black: Co^{1+}Cbl, gray: Co^{1+}Cbi). The horizontal line in (b) indicates the biological redox gap corresponding to the reduction potential difference between the MetH-bound Co^{2+}Cbx (−490 mV vs. SHE) and the physiological reducing agents (−440 mV vs. SHE) as discussed in Ref. [10].

noticed when the **H**-bonded conformation of Co^{1+}Cbx was employed (Supporting Information, Table S19), which is appreciably higher than the redox gap (50 mV vs. SHE) between the MetH-bound Co^{2+}Cbx cofactor and the physiological reducing agents.[10] This finding strongly suggests that the Co^{1+}···H interaction-driven H-bonded conformation of Co^{1+}Cbx can play a deterministic role in explaining how Co^{2+}/Co^{1+} reduction is accomplished inside MetH enzyme. This reveals a novel catalytic strategy that might not only be deployed by MetH enzyme[1] during its reactivation cycle,[13] but also by other methyltransferases[2,3] and a number of ACAs.[4,5] The axial H136 ligand in the case of MtaBC enzyme is located 2.51 Å from the Co^{2+} ion[2] and hence can serve as a potential H-bond donor for Co^{1+}···H bond formation. Similarly, in the case of PduO-type ACA, the topological location of F112 residue (3.8 Å from the metal center)[42] also makes it an ideal H donor to effect Co^{1+}···H bond formation. Furthermore, the stability of such Co^{1+}···H linkages, when formed inside the enzymes, may be enhanced through the cooperativity effect exerted by the local protein environment. For example, the axial H_2O ligand, in the case of MetH enzyme, is engaged in extensive H-bond formation with the local protein domain (the active-site Y1139 and E1097 residues;[13] Supporting Information, Figure S9) and this H-bonded network may play a crucial role in stabilizing Co^{1+}···H interaction.

In summary, the presented computational study suggests the existence of an unanticipated Co^{1+}···H linkage that has charge-transfer, correlation, dispersion, and electrostatic components. Such Co^{1+} ion-induced H-bonds can potentially fine-tune the thermodynamics of the Co^{2+}/Co^{1+} process, an indispensable chemical motif in a wide body of methyltransferases and adenosyltransferases.

Received: January 19, 2011
Revised: April 26, 2011
Published online: July 26, 2011

Keywords: cobalt · density functional calculations · hydrogen bonds · redox chemistry · transferases

[1] C. W. Goulding, D. Postigo, R. G. Matthews, *Biochemistry* **1997**, *36*, 8082 – 8091.
[2] C. H. Hagemeier, M. Kruer, R. K. Thauer, E. Warkentin, U. Ermler, *Proc. Natl. Acad. Sci. USA* **2006**, *103*, 18917 – 18922.
[3] S. W. Ragsdale, H. G. Wood, *J. Biol. Chem.* **1985**, *260*, 3970 – 3977.
[4] J. C. Escalante-Semerena, S.-J. Suh, J. R. Roth, *J. Bacteriol.* **1990**, *172*, 273 – 280.
[5] C. B. Bauer, M. V. Fonseca, H. M. Holden, J. B. Thoden, T. B. Thompson, J. C. Escalante-Semerena, I. Rayment, *Biochemistry* **2001**, *40*, 361 – 374.
[6] D. Lexa, J.-M. Savéant, *J. Am. Chem. Soc.* **1976**, *98*, 2652 – 2658.
[7] H. Vetter, Jr., J. Knappe, *Hoppe Seylers Z. Physiol. Chem.* **1971**, *352*, 433 – 446.
[8] K. R. Wolthers, N. S. Scrutton, *FEBS J.* **2009**, *276*, 1942 – 1951.
[9] M. D. Liptak, T. C. Brunold, *J. Am. Chem. Soc.* **2006**, *128*, 9144 – 9156.
[10] M. D. Liptak, S. Datta, R. G. Matthews, T. C. Brunold, *J. Am. Chem. Soc.* **2008**, *130*, 16374 – 16381.
[11] T. A. Stich, N. R. Buan, T. C. Brunold, *J. Am. Chem. Soc.* **2004**, *126*, 9735 – 9749.
[12] T. A. Stich, M. Yamanishi, R. Banerjee, T. C. Brunold, *J. Am. Chem. Soc.* **2005**, *127*, 7660 – 7661.
[13] M. Koutmos, S. Datta, K. A. Pattridge, J. L. Smith, R. G. Matthews, *Proc. Natl. Acad. Sci. USA* **2009**, *106*, 18527 – 18532.
[14] J. Kozelka, J. Berges, R. Attias, J. Fraitag, *Angew. Chem.* **2000**, *112*, 204 – 207; *Angew. Chem. Int. Ed.* **2000**, *39*, 198 – 201.
[15] S. Rizzato, J. Berges, S. A. Mason, A. Albinati, J. Kozelka, *Angew. Chem.* **2010**, *122*, 7602 – 7605; *Angew. Chem. Int. Ed.* **2010**, *49*, 7440 – 7443.
[16] A. J. Martin, *Chem. Educ.* **1999**, *76*, 578 – 583.
[17] L. Brammer, *Dalton Trans.* **2003**, 3145 – 3157.
[18] A. Albinati, F. Lianza, P. S. Pregosin, B. Muller, *Inorg. Chem.* **1994**, *33*, 2522 – 2526.
[19] K. P. Jensen, *J. Phys. Chem. B* **2005**, *109*, 10505 – 10512.
[20] N. Kumar, M. Alfonso-Prieto, C. Rovira, P. Lodowski, M. Jaworska, P. M. Kozlowski, *J. Chem. Theory Comput.* **2011**, *7*, 1541 – 1551.
[21] B. Kräutler, W. Keller, C. Kratky, *J. Am. Chem. Soc.* **1989**, *111*, 8938 – 8940.
[22] J. T. Jarrett, S. Huang, R. G. Matthews, *Biochemistry* **1998**, *37*, 5372 – 5382.
[23] S. J. Grimme, *J. Comput. Chem.* **2006**, *27*, 1787 – 1799.
[24] J. D. Chai, M. Head-Gordon, *Phys. Chem. Chem. Phys.* **2008**, *10*, 6615 – 6622.
[25] A. D. Becke, *J. Chem. Phys.* **1986**, *84*, 4524 – 4529.
[26] J. P. Perdew, *Phys. Rev. B* **1986**, *33*, 8822 – 8824.
[27] A. D. Becke, *J. Chem. Phys.* **1997**, *107*, 8554 – 8560.
[28] F. A. Hamprecht, A. J. Cohen, D. J. Tozer, N. C. Handy, *J. Chem. Phys.* **1998**, *109*, 6264 – 6271.
[29] H. L. Schmider, A. D. Becke, *J. Chem. Phys.* **1998**, *108*, 9624 – 9631.
[30] J.-D. Chai, M. Head-Gordon, *J. Chem. Phys.* **2008**, *128*, 084106.
[31] W. Yao, O. Eisenstein, R. H. Crabtree, *Inorg. Chim. Acta* **1997**, *254*, 105 – 111.
[32] K. Wiberg, *Tetrahedron* **1968**, *24*, 1083.
[33] R. Lonsdale, J. N. Harvey, A. J. Mullholand, *J. Phys. Chem. Lett.* **2010**, *1*, 3232 – 3237.
[34] R. A. Moss, L. Wang, C. M. Odorisio, K. Krogh-Jespersen, *J. Am. Chem. Soc.* **2010**, *132*, 10677 – 10679.
[35] D. Lexa, J.-M. Savéant, *Acc. Chem. Res.* **1983**, *16*, 235 – 243.
[36] R. F. W. Bader, *Atoms in Molecules: A Quantum Theory*, Oxford University Press, New York, **1990**.
[37] A. E. Reed, L. A. Curtiss, F. Weinhold, *Chem. Rev.* **1988**, *88*, 899 – 926.
[38] M. Iwaoka, H. Komatsu, T. Katsuda, S. Tomoda, *J. Am. Chem. Soc.* **1996**, *118*, 8077 – 8084.
[39] M. Iwaoka, H. Komatsu, T. Katsuda, S. Tomoda, *J. Am. Chem. Soc.* **2004**, *126*, 5309 – 5317.
[40] M. Iwaoka, H. Komatsu, T. Katsuda, S. Tomoda, *J. Am. Chem. Soc.* **2002**, *124*, 1902 – 1909.
[41] M. Kumar, P. M. Kozlowski, *unpublished results.*
[42] P. E. Mera, M. C. Maurice, I. Rayment, J. C. Escalante-Semerena, *Biochemistry* **2009**, *48*, 3138 – 3145.

